Glycosylation with *O*-Linked β-N-acetylglucosamine (*O*-GlcNAc) induces vascular dysfunction via production of superoxide anion / reactive oxygen species.

[*] Leonardo Souza-Silva [a]; [*] Rheure Alves-Lopes [b,c]; Jéssica Silva Miguez [a]; Vanessa Dela Justina [a], Karla Bianca Neves [b,c]; Fabíola Leslie Mestriner [b]; Rita de Cassia Tostes [b]; Fernanda Regina Giachini [a]; Victor Vitorino Lima [a]

[*] *The authors equally contribute to this manuscript.*

[a] *Institute of Biological and Health Sciences, Federal University of Mato Grosso, Barra do Garças, MT, Brazil.*

[b] *Department of Pharmacology, Ribeirao Preto Medical School, University of São Paulo, Ribeirao Preto, Brazil.*

[c] *Institute of Cardiovascular and Medical Sciences, BHF Glasgow Cardiovascular Research Centre, University of Glasgow, UK.*

Running Title: *O*-GlcNAc, ROS and vascular dysfunction.

Corresponding author:

Victor Vitorino Lima, Ph.D.

Federal University of Mato Grosso

Institute of Biological and Health Sciences

Av. Valdon Varjao. Barra do Garças - Mato Grosso. 78600-000

Phone: +55-66-3402-1100 / +55-66-3402-

E-mail: vvlima@ufmt.br

ABSTRACT

Overproduction of superoxide anion ($\bullet O_2^-$) and *O*-linked β-N-acetylglucosamine (*O*-GlcNAc)-modification in the vascular system are contributors to endothelial dysfunction. This study tested the hypothesis that increased levels of *O*-GlcNAc-modified proteins contribute to $\bullet O_2^-$ production via activation of NADPH oxidase, resulting in impaired vasodilation. Rat aortic segments and vascular smooth muscle cell (VSMCs) were incubated with vehicle (methanol) or PUGNAc (100 μM). PUGNAc produced a time-dependent increase in *O*-GlcNAc levels in VSMC and decreased endothelium-dependent relaxation, which was prevented by apocynin and Tiron, suggesting that $\bullet O_2^-$ contributes to endothelial dysfunction under augmented *O*-GlcNAc levels. Aortic segments incubated with PUGNAc also exhibited increased levels of (ROS), assessed by dihydroethidium fluorescence, and augmented $\bullet O_2^-$ production, determined by lucigenin-enhanced chemiluminescence. Additionally, PUGNAc treatment increased Nox1 and Nox4 protein expression in aorta and VSMCs. Translocation of $p47^{phox}$ subunit from the cytosol to the membrane was greater in aortas incubated with PUGNAc. VSMCs displayed increased $p22^{phox}$ protein expression after PUGNAc incubation, suggesting that NADPH oxidase is activated in conditions where *O*-GlcNAc protein levels are increased. In conclusion, *O*-GlcNAc levels reduce endothelium-dependent relaxation by overproduction of $\bullet O_2^-$ via activation of NADPH oxidase. This may represent an additional mechanism by which augmented *O*-GlcNAc levels impair endothelial and vascular function.

Key words: posttranslational modification, oxidative stress, vascular reactivity, vasodilation, PUGNAc.

INTRODUCTION

Superoxide anion ($\bullet O_2^-$) is a key reactive oxygen species (ROS) that plays both physiological and pathological roles on cellular redox signaling. Excessive production of $\bullet O_2^-$ has deleterious effects in the vascular system, contributing to vascular dysfunction (Munzel et al. 2002; Rabelo et al. 2010; Brieger et al. 2012). Accordingly, oxidative stress associated with hyperglycemia not only amplifies inflammation-related events but also worsens endothelial dysfunction. ROS also increase flux in the hexosamine biosynthetic pathway (HBP), favoring uridine 5′-diphospho-N-acetylglucosamine (UDP-GlcNAc) synthesis (Rajapakse et al. 2009).

Glycosylation with *O*-Linked β-N-acetylglucosamine (*O*-GlcNAc) on serine and threonine residues of nuclear and cytoplasmic proteins is a post-translational modification that alters the function of numerous proteins important in vascular function. It is estimated that between 2% to 5% of the total glucose entering the cell is metabolized via HBP, culminating in the formation of UDP-GlcNAc, the substrate for *O*-GlcNAc protein modification (Love et al. 2005; Ngoh et al. 2011).

Augmented *O*-GlcNAc levels were described to impair endothelial function in penile tissue, due inactivation of phosphorylated endothelial nitric oxide synthase (eNOS), in diabetes-associated erectile dysfunction (Musicki et al. 2005). Impaired endothelial-dependent relaxation along with increased *O*-GlcNAcylation was also observed in the vasculature in normoglycemic conditions (Lima et al. 2008), resulting in eNOS-glycosylation (Lima et al. 2009). Yet, inducible nitric oxide synthase (iNOS) is also suppressed by O-GlcNAc, abolishing acute vascular dysfunction induced by tumor necrosis factor alpha (TNF-α) (Hilgers et al. 2012).

In cardiomyocytes, increased levels of *O*-GlcNAc-modified proteins decrease ROS formation during ischemia/reperfusion, favoring cell survival (Ngoh et al. 2011). In

opposition, in an experimental model of diabetes, high levels of *O*-GlcNAc proteins create a pro-oxidative environment in the liver (Dinić et al. 2013). Additionally, *O*-GlcNAc inhibition by blocking the rate-limiting enzyme glutamine, fructose-6-phosphate aminotransferase (GFAT) prevents endothelial dysfunction in cells isolated from human umbilical veins submitted to hyperglycemic conditions. This effect is associated with improvement of antioxidant defenses (Rajapakse et al. 2009). The exactly mechanisms by which *O*-GlcNAc interferes with ROS production, and vice-versa, remains a paradox.

Taking into acount that both augmented *O*-GlcNAc levels and increased ROS generation alter vascular function, favoring endothelial dysfunction, we tested the hypothesis that increased *O*-GlcNAc levels augment $\bullet O_2^-$ generation via NADPH oxidase activation, resulting in impaired endothelium-dependent vasodilation.

MATERIALS AND METHODS

Animals

Male, 14-16 weeks-old Wistar rats were used in the experimental protocols (n = 4-6 for each experimental group). The animals were housed in high-top-filter cages (3 rats per cage – 48.3 x 33.7 x 25.3 cm) in a room with controlled humidity (45 ± 5 %) and temperature (21 ± 2°C), and light/dark cycles of 12 h. Animals had free access to food (commercially available standard rat chow, Purina) and potable tap water. All experimental procedures were approved by the Ethics Committee on Animal Experiments of the Ribeirao Preto Medical School, University of Sao Paulo (protocol 013/2013) and are in accordance with the Guidelines of the Brazilian College of Animal Experimentation (COBEA) and with the the Guide for the Care and Use of Laboratory Animals, from the National Academic Press, 1996.

Tissue Preparation

Rats were euthanized in a carbon dioxide (CO_2) chamber and the thoracic aorta was rapidly removed and cleaned of fat and connective tissue in an ice-cold Krebs solution containing the following salts (in mM): NaCl, 130; $NaHCO_3$, 14.9; KCI, 4.7; KH_2PO_4, 1.18; $MgSO_4 \cdot 7H_2O$, 1.18; $CaCl_2 \cdot 2H_2O$, 1.56; EDTA, 0.026; glucose, 5.5. Aortic segments were placed in culture multiwell plates containing 5 mL of Dulbecco's Modified Eagle Medium (DMEM) (GIBCO-BRL, Gaithersburg, MD, USA) supplemented with 10% fetal bovine serum (FBS) and 1% penicillin and streptomycin. Segments were incubated with vehicle (methanol, 40 uL) or O-(2-Acetamido-2-deoxy-D-glucopyranosylidenamino) N-phenylcarbamate **(**PUGNAc; 100 µM), in the presence or absence of apocynin (100 µM, NADPH oxidase inhibitor) or Tiron (100 µM, $\bullet O_2^-$ scavenger). Incubations were performed

for 6, 12 or 24 h, in a humidified incubator at 37º C and gassed constantly with 95% O_2 and 5% CO_2.

VSMCs isolation and culture

Vascular smooth muscle cells (VSMCs) were isolated from rat thoracic aortas, by the explant technique, as previously described (Ross 1971). Cultures were maintained in DMEM (GIBCO-BRL, Gaithersburg, MD, USA) supplemented with 10% FBS (Invitrogen, Grand Island, NY, USA) and 1% penicillin and streptomycin. After maximum confluence and 24 h removal of serum, cells were incubated with vehicle (methanol) or PUGNAc (100 μM) for 6, 12 or 24 h. Only fourth-passage cells were used in all experiments. VSMCs were identified by determination of α-actin expression by fluorescence microscopy, and the absence of endothelial cells was confirmed by assessment of von Willebrand factor by real-time polymerase chain reaction (RT-PCR; data not shown).

Immunofluorescence microscopy analysis

O-GlcNAc levels were evaluated in VSMC plated on glass coverslips (5000 cells/cm). After 24 h in serum-free media, VSMC were incubated with vehicle or PUGNAc (100 μM), for 24 h. Cells were washed, fixed in 4 % paraformaldehyde for 10 min, permeabilized (0.1 % Nonidet P40) and incubated in blocking buffer [1 % (w/v) BSA in PBS] for 30 min at room temperature (25° C). Cells were incubated with the primary antibody mouse anti-*O*-GlcNAc (1:100 dilution), for 1 h at 37° C and counterstained with a FITC-conjugated anti-(mouse IgG) secondary antibody (1:500 dilution; Jackson Immunochemistry) at 4° C overnight. Cells were then incubated with 4 ,6-diamidino-2-phenyindole (DAP; Sigma) for 20 min to detect nuclei. Coverslips were mounted, and labeled cells were examined using a Zeiss microscope and software.

Dihydroethidium fluorescence assay

Dihydroethidium (DHE), an indicator of ROS generation, was used in this study as previously described (Chignalia et al. 2012). Aortic segments were isolated and incubated with vehicle, PUGNAc (12 or 24 h), or Angiotensin II (1 μM; 30 min, positive control) in Krebs solution with controlled temperature (37ºC), continuously gassed with a gas mixture containing CO_2 (5%) and O_2 (95%). Thereafter, segments of aorta were embedded in tissue freezing medium snap-frozen and placed in a freezer at -70ºC. The 10μm thick cryosections were placed on individual glass slides using Cryostat. At the day of the experiment, cryosections were incubated in a light-protected and humidified chamber with PBS (37°C, 30 min). After this period, DHE (50 mM in PBS) was topically applied to each tissue section (37ºC, for 30 min). The images were obtained at excitation/emission (nm) 518/605, using an optical microscope (Eclipse 80i, Nikon, Japan) using a 20X objective. The results are reported as fold of change and compared to the control group.

Lucigenin-enhanced chemiluminescence

Aortic segments were stimulated with vehicle or PUGNAc (for 12 or 24 h), in culture conditions. After stimulation, aortas were washed and harvested in lysis buffer [KH_2PO_4, 20 mM; EGTA 1, mM; aprotinin, 1 μg/mL; leupeptin 1, μg/mL; pepstatin, 1 μg/mL; and phenylmethylsulfonyl fluoride (PMSF), 1 mM]. Following, 50 μL of the sample were added to a suspension containing 175 μL of assay buffer [KH_2PO_4, 50 mM; EGTA, 1 mM; and sucrose, 150 mM; (pH 7.4)] and lucigenin (5 μM). NADPH (1 μM) was added to the suspension (300 μL) containing lucigenin.

Luminescence was measured every 18 seconds for 3 min by a luminometer (AutoLumat LB 953, Berthold), before and after stimulation with NADPH. A buffer blank

was subtracted from each reading. The results are expressed as counts per milligram of protein and as a percentage of control).

Western Blotting

Proteins (60 µg) extracted from aorta or VSMCs were separated by electrophoresis, and Western blots performed as previously described (Lima et al. 2008). Antibodies used were: anti-O-GlcNAc antibody (1:2000; Pierce Biotechnology); anti-Nox1, anti-Nox4, anti-$p47^{phox}$ or anti-$p22^{phox}$ primary antibodies (1:1000 each; ProSci), incubated for a period of 24 h, at 4 ºC, under constant agitation. After, incubation with the respective secondary antibodies was performed and signals were developed with chemiluminescence, visualized by autoradiography, and quantified densitometrically. β-actin [(1:10000), Sigma-Aldrich, Inc.] was used as a housekeeping protein. Results were normalized to β-actin protein and expressed as arbitrary units.

Membrane and cytosol fractionation by ultracentrifugation

The expression of NADPH oxidase $p47^{phox}$ subunit was determined in membrane and cytosol fractions. Differential centrifugation was used to obtain the membrane and cytoplasmic fractions. After incubation with vehicle or PUGNAc (12 h), frozen aortic segments were mechanically pulverized and the resulting powder collected in 1.5 mL plastic tubes. Thereafter, cell lysis buffer was added and samples were centrifuged (30,000 G, for 20 min at 4 ºC). The supernatant (corresponding to the cytosolic fraction) was removed, and the pellet was resuspended in modified lysis buffer (KH_2PO_4, 20 mM; EDTA, 1 mM; aprotinin, 10 g/mL; leupeptin, 0.5 g/mL; pepstatin, 0.75 g/mL; PMSF, 0.5 mM; and Triton 1%). The pellet (membrane fraction) was resuspended in this solution and then incubated on

ice for 30 min with intermittent vortex. The determination of protein concentration was performed in both fractions by Bradford method.

Translocation of p47^{phox}

Expression of p47^{phox} in cell fractions was determined by Western blot. The ratio between the expression of p47^{phox} in the membrane and cytosolic fractions, used as an index of NADPH oxidase activation, was determined using primary anti-p47^{phox} antibody [ProSci, (1:1000 dilution), 24 h incubation, at 4 °C, under constant agitation]. Results were normalized by expression of the protein in the cytosolic fraction, and expressed as arbitrary units.

Vascular Reactivity

Vascular function was assessed in thoracic aorta segments (4 mm in length), after incubation with vehicle or PUGNAc, in the presence or absence of apocynin or Tiron (24 h). Vascular segments were mounted in myograph chambers (Mulvany-Halpern, model 610M, Danish Myotech, Aarhus, Denmark) for isometric tension measurements. Vascular reactivity was determined using a data acquisition system (PowerLab 8/SP - ADInstruments Pty Ltd, Colorado Springs, USA). Basal tension of the aortic rings were set to 30 mN, and thereafter, followed by a stabilization period of 60 min in Krebs solution at 37ºC, continuously gassed with a gas mixture containing CO_2 (5%) and O_2 (95%). Blood vessel integrity was determined using KCl (120 mM). Endothelium-dependent relaxation was assessed by measuring the relaxation response to acetylcholine (ACh: 1 nM to 100 µM) in PE-contracted vessels (10 µM).

Statistical analysis

The results are presented as mean ± SEM (n), where "n" is relative to number of animals used in experiments. The concentration-response curves were fit using a nonlinear fitting interactive program (Graph Pad Prism 3.0, GraphPad Software Inc., San Diego, CA) and two pharmacological parameters were obtained: the maximum effect produced by the agonist (or E_{max}) and -log EC_{50} (or pD_2). Statistical analysis of the pD_2 and E_{max} values were calculated. Statistical analysis of the pD_2 and E_{max} values was calculated. Statistics were conducted using Student t test or one-way analysis of variance, followed by post-hoc comparisons using the Newman-Keuls test, as indicated in the legends. Values of $P < 0.05$ were considered statistically significant.

RESULTS

O-Glc*NAc, ROS and endothelium-dependent relaxation response*

PUGNAc is a potent inhibitor of O-GlcNAcase and was used to increase O-GlcNAc protein levels, aiming to investigate the role of O-GlcNAcylation in the vascular function (Lima et al. 2009; Lima et al. 2011; Lima et al. 2011). PUGNAc incubation effectively increased global *O*-GlcNAc levels in VSMC after 6 and 24 hours (Figure 1A). O-GlcNAc was also augmented after 12 hours of PUGNAC incubation, compared to vehicle, in a similar manner that 24 hours (data not shown). Treatment of VSMCs with PUGNAc (100μM) for 24 hours was also determined by immunohistochemistry, where *O*-GlcNAcylation was still augmented (Figure 1B).

Endothelium-dependent relaxation was assessed by performing concentration-response curves to ACh in aortas incubated with vehicle (methanol) or PUGNAc (for 12 or 24 h), in the absence or presence of apocynin (NADPH inhibitor, 24 h) or Tiron ($\bullet O_2^-$ scavenger, 24 h). No differences in the endothelium-dependent relaxations were observed in aortas treated with PUGNAc (E_{max} 88.7 ± 9%; pD_2 5.9 ± 0.3) or vehicle (E_{max} 87.5 ± 6.5%; pD_2 6.2 ± 0.2) for 12 h. However, PUGNAc incubation for 24 h decreased ACh-induced relaxation (E_{max} 77.8 ± 3.1%; pD_2 6.6 ± 0.1), compared to aortas incubated with vehicle (E_{max} 94.1 ± 1.9%; pD_2 7.3 ± 0.07).

No differences were observed in vascular reactivity to ACh in aortas treated with PUGNAc plus apocynin (E_{max} 86.8 ± 2.2%; pD_2 7.5 ± 0.1), when compared to vehicle-incubated aortas, suggesting that NADPH oxidase inhibition prevented vascular dysfunction under conditions of augmented O-GlcNAc (Figure 2; Table 1). Similar results were observed when aortas were simultaneously incubated with PUGNAc and Tiron (E_{max} 88.0 ± 2.5%; pD_2 7.2 ± 0.1), showing that $\bullet O_2^-$ removal by a scavenger agent prevented the decreased ACh relaxation induced by high levels of O-GlcNAc proteins (Figure 2; Table 1).

O-Glc*NAc induces ROS generation*

Dihydroethidium staining and lucigenin-enhanced chemiluminescence assays were used to elucidate whether O-GlcNAc increases ROS generation in rat aortas (Figures 3A-B and 3C, respectively).

Treatment with PUGNAc for 12 and 24 h significantly increased vascular ROS production, compared to vehicle treatment. Additionally, PUGNAc produced a transient increase of ROS production, since ROS production was lower in aortas treated with PUGNAc for 24 h, when compared to 12 h. Ang II (30 min) was used as a positive control in the DHE assay. As expected, aortas treated with Ang II displayed elevated levels of ROS (Figures 3A-B).

Aortas treated with PUGNAc for 12 h, but not for 24 h, displayed increased production of $\bullet O_2^-$, as determined by lucigenin-enhanced chemiluminescence and compared to the respective vehicle group (Figure 3C).

O-Glc*NAc protein levels and NADPH oxidase expression/activity*

Protein expression of Nox-1, Nox-4, $p47^{phox}$ and $p22^{phox}$ was determined to investigate whether NADPH oxidase plays a role in ROS production induced by high levels of O-GlcNAc. Nox-1 and Nox-4 protein expression was increased after treatment with PUGNAc for 12 h in aortas (Figures 4A and 4B) and VSMCs (Figures 4C and 4D). Nox-1 expression (Figure 4A), but not Nox-4 expression (Figure 4B), was increased in aortas incubated with PUGNAc for 6, 12 and 24 h when compared to that in the control group. These results show that increased *O*-GlcNAc proteins levels, in aorta as well as in VSMCs, modulate the expression of both Nox-1 and Nox-4.

PUGNAc incubation (12 h) augmented $p47^{phox}$ membrane translocation (Figure 5), strongly suggesting that increased O-GlcNAc levels leads to NADPH oxidase activation. Furthermore, we determined $p22^{phox}$ protein expression, which is essential for NADPH

oxidase activation in VSMC. After PUGNAc incubation for 12h, but not for 6 or 24 h, $p22^{phox}$ protein expression was increased in VSMCs (Figure 6).

DISCUSSION

Recent interest has been devoted to the modulatory effects of *O*-GlcNAc in the vasculature, since several signaling pathways that control vascular function are targets for *O*-GlcNAc modifications (Hart et al. 2007; Laczy et al. 2009; Lima et al. 2009), as well as by ROS (Munzel et al. 2002; Rabelo et al. 2010; Brieger et al. 2012). In order to investigate whether increased levels of *O*-GlcNAc-modified proteins contribute to $\bullet O_2^-$ production via activation of NADPH oxidase, resulting in impaired vasodilation, the experimental design included strategies to increase *O*-GlcNAc protein levels in aortas and VSMCs and to determine whether *O*-GlcNAcylation effects on vascular function are mediated by ROS.

The major finding of this study was that increased levels of O-GlcNAc, resulting from OGA inhibition by PUGNAc, culminated in endothelial dysfunction, at least in part by a mechanism dependent on $\bullet O_2^-$ overproduction. This fact was reinforced by vascular functional studies using Apocynin and Tiron, which prevented endothelial dysfunction caused by increased O-GlcNAc. Apocynin, an inhibitor of NADPH oxidase, inhibits Nox-1 and Nox-4, decreasing the production of $\bullet O_2^-$ and subsequent generation of others ROS. Apocynin has been shown to reduce ROS in various cell types, including VSMC (Touyz et al. 2008), to inhibit NADPH oxidase complex in aortas from diabetic rats (Rehman et al. 2013), and to restore endothelial function in diabetic rats (Olukman et al. 2010; Taye et al. 2010). Tiron is a recognized non-toxic chelating agent and membrane-permeable antioxidant, which selectively removes $\bullet O_2^-$. Tiron also inhibits apoptosis mediated by increased ROS levels (Yamada et al. 2003; Yang et al. 2007).

Indeed, increased levels of O-GlcNAc proteins in aortic segments from Wistar rats lead to increased production of $\bullet O_2^-$, as demonstrated by DHE stain. Activation of the HBP, which increases the production of UDP-GlcNAc and stimulates O-GlcNAc modification of proteins, has been shown to induce ROS generation and oxidative stress in mesangial cells

(Singh et al. 2007). Increased O-GlcNAc proteins also promote ROS production in renal mesangial cells incubated in high glucose conditions, or upon glucosamine stimulation (Goldberg et al. 2011). Furthermore, accumulation of advanced glycation end products triggers ROS generation and nuclear O-GlcNAc activation in cardiac myocytes (Li et al. 2007).

Of importance, O-GlcNAc-induced ROS production peaked at 12 h, the same time frame observed for $\bullet O_2^-$ production which relied on NADPH oxidase activity. The NADPH oxidase complex is a major source of $\bullet O_2^-$ present in vascular cells and has membrane-bound subunits (Nox-1, Nox-2, Nox-4 and Nox-5, $p22^{phox}$) and cytosolic subunit ($p47^{phox}$, $p67^{phox}$) (Martinez-Revelles et al. 2013). Nox-1 and Nox-4 expression in VSMC and aorta, as well as $p22^{phox}$ subunit in VSMC, also peaked at 12 h.

It is known that Nox-1 activity and, consequently, the production of $\bullet O_2^-$ is regulated by the subunit $p47^{phox}$ and $p22^{phox}$ (Geiszt 2006; Lassegue et al. 2012), since the $p22^{phox}$ and $p47^{phox}$ subunits are essential for the activity of NADPH oxidase, in VSMC (Niu et al. 2010). Nox-4 activation requires only association with $p22^{phox}$ subunit (Ambasta et al. 2004; Martyn et al. 2006), not being controlled by the cytosolic subunits of the NADPH oxidase (Martyn et al. 2006), and $p22^{phox}$ subunit is required to generate a Nox-4-dependent radical (Ambasta et al. 2004). Our results demonstrate that increased production of $\bullet O_2^-$ upon PUGNAc stimulation is due to increased levels of O-GlcNAc, through increased protein expression of Nox-1 and Nox-4 enzymes. Furthermore, O-GlcNAcylation increased $p22^{phox}$ protein expr**essi**on after 12 h of PUGNAc incubation.

Zachara and colleagues, in 2016,{Lee, 2016 #774} elegantly showed that oxidative stress induces O-GlcNAcylation. Indeed, these authors discussed that O-GlcNAcylation is one component of the cellular stress response that is relevant to a variety of models of injury in several cell lines and tissue types, and upon oxidative stress proteins related to cellular

injury. Here, we showed, in a humbler manner, the opposite direction of this same equation. We demonstrated that increased O-GlcNAcylation may induce oxidative stress. Besides de subunits of NADPH oxidase were increased after PUGNAC incubation, one possibility was that activity of this enzyme may or not be altered. Of importance, translocation of $p47^{phox}$ subunit was also assessed at 12 h, demonstrating increased activity of NADPH after 12 h of PUGNAc incubation in aorta. Evidence suggests that phosphorylation of the three serine residues in $p47^{phox}$ is crucial for translocation of the cytosolic components and assembly of the active NADPH oxidase (Johnson et al. 1998; Ago et al. 1999).

Many phosphorylation sites are also known glycosylation sites, and this mutual assignment can produce different activities or change the stability of the target protein (Hart et al. 1995; Hart et al. 1996; Hu et al. 2010; Zeidan et al. 2010). In this sense, Goldberg and colleagues (2011) speculated that O-GlcNAc increases the phosphorylation of the NADPH oxidase subunit $p47^{phox}$, through p38 MAPK activation, and up-regulates the expression of the NADPH oxidase subunit Nox4, in glomerular mesangial cells (Goldberg et al. 2006). It remains to be elucidated whether $p22^{phox}$ is a target for O-GlcNAc.

ROS are produced in several cells of the cardiovascular system, including cardiac myocytes, endothelial and smooth muscle cells and are tightly regulated by antioxidants and oxidants including hydrogen peroxide (H_2O_2), $\bullet O_2^-$, hydroxyl radical (OH^-), among others (Touyz et al. 2008; Silva et al. 2013). Under oxidative stress, ROS production can lead to endothelial dysfunction, by decreasing NO, which reacts with $\bullet O_2^-$ to form $\bullet ONOO^-$ (Li et al. 2005; Silva et al. 2013), increases contractility, vascular smooth muscle cell growth, monocyte migration, lipid peroxidation, inflammation, and other processes contributing to cardiovascular damage (Pashkow 2011; Satoh et al. 2011; Touyz et al. 2011).

Since $\bullet O_2^-$ production was increased by augmented *O*-GlcNAc levels, and endothelium-dependent relaxation was decreased, one may speculate that this radical may be

reacting with NO, thereby contributing to impaired endothelium-dependent relaxation under PUGNAc treatment. In fact, decreased endothelial-dependent relaxation observed in this study does not appears to be exclusively dependent on decreased availability of NO. By evaluating the effects of PUGNAc in a time-course manner, one can observed that the peak of $\bullet O_2^-$ overproduction occurs at 12 hours, and that ROS production is maintained for 24 hours, whereas endothelium-dependent relaxation is decreased only after 24 hours. This may indicate that $\bullet O_2^-$ overproduction, via NADPH oxidase activation, is an initial and essential event to increase ROS production, resulting in vascular dysfunction.

On this regard, the enhancement of $\bullet O_2^-$ significantly contributes to the instability of endothelium derived relaxation factors (EDRF), as initially demonstrated by Moncada and colleagues in 1986 (Gryglewski, Palmer et al. 1986). Here, vascular function wass initially challenged by an oxidative burst at 12 hours, with massive production of $\bullet O_2^-$. In the other hand, the impairment of endothelium-dependent relaxation occurred in a different time-frame than oxidative stress enhancement, and was observed after 24 hours, but still prevented by anti-oxidant drugs. One possibility is that besides the short half-life of $\bullet O_2^-$, this anion rapidly combines with NO to form more stable products, such as $ONOO^-$, a potent cytotoxic oxidant, which may cause oxidative damage in endothelial cells through several mechanisms including nitration of tyrosine residues of proteins, peroxidation of lipids, degradation of DNA, oligonucleosomal fragments, among others (Hemnani and Parihar 1998).

Another possibility, not addressed here, is that O-GlcNAc may affect anti-oxidant mechanism, and even if $\bullet O_2^-$ production was recovered after 24 hours, this protective cellular mechanism may still be disrupted. For example, glutathione peroxidase 1, an anti-oxidant enzyme, is modified with O-GlcNAc on its C-terminus in rat VSMCs and HEK293 cells, under hyperglycemic conditions (Yang, Park et al. 2010). Still, other possibility is that

other sources of $\bullet O_2^-$ production, for example the uncoupling of eNOS, may be activated over 24 hours (Karbach, Wenzel et al. 2014).

Considerable data have shown that O-GlcNAc regulates cellular stress responses, favoring cell survival (Groves et al. 2013). Of importance, inhibition of OGA with PUGNAc significantly reduced ROS in rat cardiomyocytes, (Ngoh et al. 2011) corroborating data showing that O-GlcNAc seems to be protective in the heart. Several aspects must be considered in this interplay between O-GlcNAc and ROS generation: acute vs. chronic effects of O-GlcNAcylation, the initial cellular conditions when components of the O-GlcNAc system are manipulated, global vs. localized increases of O-GlcNAcylation and the specific proteins that are O-GlcNAc-modified in different tissues.

The results show here also suggest that other mechanisms are involved in the critical interplay between O-GlcNAcylation and ROS generation, in the cardiovascular system. Indeed, evidence from the literature, along with our data, strongly suggests an interplay between O-GlcNAcylation and ROS generation, and vice-versa, in the cardiovascular system. Hence, both ROS and O-GlcNAc are crucial, not only to control vascular function in physiological conditions, but also under pathological states where ROS and O-GlcNAc are enhanced, culminating in cellular injury and organ dysfunction. Future studies, evaluating other ROS products, as well as other sources of ROS, will contribute to the understanding of the relationship between ROS and *O*-GlcNAc and whether this interplay also occurs in *in vivo* conditions.

ACKNOWLEDGMENTS

This work was supported in part by Fundação de Amparo à Pesquisa do Estado de Mato Grosso [grant number 151371/2014 (to FRG) and 211917/2015 (to VVL)], Coordenação de Aperfeiçoamento de Pessoal de Nível Superior [grant number 23038009165/2013-48 (to VVL)], Fundação de Amparo à Pesquisa do Estado de São Paulo [grant number 2008/58142-7 to RCT and 2013/08216-2 to the Center of Research on Inflammatory Diseases - CRID)] and Conselho Nacional de Desenvolvimento Científico e Tecnológico [445777/2014-1 (to VVL) and 471675/2013/0 (to FRC)]. We would also like to thank the technical staff from our laboratories that contributed to the studies.

CONFLICT OF INTEREST

None declared.

REFERENCES

Ago, T., Nunoi, H., Ito, T. and Sumimoto, H. 1999. Mechanism for phosphorylation-induced activation of the phagocyte NADPH oxidase protein p47(phox). Triple replacement of serines 303, 304, and 328 with aspartates disrupts the SH3 domain-mediated intramolecular interaction in p47(phox), thereby activating the oxidase. J Biol Chem. **274**(47): 33644-33653.

Ambasta, R.K., Kumar, P., Griendling, K.K., Schmidt, H.H., Busse, R. and Brandes, R.P. 2004. Direct interaction of the novel Nox proteins with p22phox is required for the formation of a functionally active NADPH oxidase. J Biol Chem. **279**(44): 45935-45941.

Brieger, K., Schiavone, S., Miller, F.J., Jr. and Krause, K.H. 2012. Reactive oxygen species: from health to disease. Swiss Med Wkly. **142**: w13659.

Chignalia, A.Z., Schuldt, E.Z., Camargo, L.L., Montezano, A.C., Callera, G.E., Laurindo, F.R., et al. 2012. Testosterone induces vascular smooth muscle cell migration by NADPH oxidase and c-Src-dependent pathways. Hypertension. **59**(6): 1263-1271.

Dinić, S., Arambašić, J., Mihailović, M., Uskoković, A., Grdović, N., Marković, J., et al. 2013. Decreased O-GlcNAcylation of the key proteins in kinase and redox signalling pathways is a novel mechanism of the beneficial effect of α-lipoic acid in diabetic liver. Br J Nutr. **110**(3): 401-412.

Geiszt, M. 2006. NADPH oxidases: new kids on the block. Cardiovasc Res. **71**(2): 289-299.

Goldberg, H., Whiteside, C. and Fantus, I.G. 2011. O-linked beta-N-acetylglucosamine supports p38 MAPK activation by high glucose in glomerular mesangial cells. Am J Physiol Endocrinol Metab. **301**(4): E713-726.

Goldberg, H.J., Whiteside, C.I., Hart, G.W. and Fantus, I.G. 2006. Posttranslational, reversible O-Glycosylation is stimulated by high glucose and mediates plasminogen activator inhibitor-1 gene expression and Sp1 transcriptional activity in glomerular mesangial cells. Endocrinology. **147**(222–231).

Groves, J.A., Lee, A., Yildirir, G. and Zachara, N.E. 2013. Dynamic O-GlcNAcylation and its roles in the cellular stress response and homeostasis. Cell Stress Chaperones. **18**(5): 535-558.

Hart, G.W., Greis, K.D., Dong, L.Y., Blomberg, M.A., Chou, T.Y., Jiang, M.S., et al. 1995. O-linked N-acetylglucosamine: the "yin-yang" of Ser/Thr phosphorylation? Nuclear and cytoplasmic glycosylation. Adv Exp Med Biol. **376**: 115-123.

Hart, G.W., Housley, M.P. and Slawson, C. 2007. Cycling of O-linked beta-N-acetylglucosamine on nucleocytoplasmic proteins. Nature. **446**(7139): 1017-1022.

Hart, G.W., Kreppel, L.K., Comer, F.I., Arnold, C.S., Snow, D.M., Ye, Z., et al. 1996. O-GlcNAcylation of key nuclear and cytoskeletal proteins: reciprocity with O-phosphorylation and putative roles in protein multimerization. Glycobiology. **6**(7): 711-716.

Hilgers, R.H., Xing, D., Gong, K., Chen, Y.F., Chatham, J.C. and Oparil, S. 2012. Acute O-GlcNAcylation prevents inflammation-induced vascular dysfunction. Am J Physiol Heart Circ Physiol. **303**(5): H513-522.

Hu, P., Shimoji, S. and Hart, G.W. 2010. Site-specific interplay between O-GlcNAcylation and phosphorylation in cellular regulation. FEBS Lett. **584**(12): 2526-2538.

Johnson, J.L., Park, J.W., Benna, J.E., Faust, L.P., Inanami, O. and Babior, B.M. 1998. Activation of p47(PHOX), a cytosolic subunit of the leukocyte NADPH oxidase. Phosphorylation of ser-359 or ser-370 precedes phosphorylation at other sites and is required for activity. J Biol Chem. **273**(52): 35147-35152.

Laczy, B., Hill, B.G., Wang, K., Paterson, A.J., White, C.R., Xing, D., et al. 2009. Protein O-GlcNAcylation: a new signaling paradigm for the cardiovascular system. Am J Physiol Heart Circ Physiol. **296**(1): H13-28.

Lassegue, B., San Martin, A. and Griendling, K.K. 2012. Biochemistry, physiology, and pathophysiology of NADPH oxidases in the cardiovascular system. Circ Res. **110**(10): 1364-1390.

Li, J., Li, W., Altura, B.T. and Altura, B.M. 2005. Peroxynitrite-induced relaxation in isolated rat aortic rings and mechanisms of action. Toxicol Appl Pharmacol. **209**(3): 269-276.

Li, S.Y., Sigmon, V.K., Babcock, S.A. and Ren, J. 2007. Advanced glycation endproduct induces ROS accumulation, apoptosis, MAP kinase activation and nuclear O-GlcNAcylation in human cardiac myocytes. Life Sci. **80**(11): 1051-1056.

Lima, V.V., Giachini, F.R., Carneiro, F.S., Carneiro, Z.N., Fortes, Z.B., Carvalho, M.H., et al. 2008. Increased vascular O-GlcNAcylation augments reactivity to constrictor stimuli - VASOACTIVE PEPTIDE SYMPOSIUM. J Am Soc Hypertens. **2**(6): 410-417.

Lima, V.V., Giachini, F.R., Carneiro, F.S., Carneiro, Z.N., Fortes, Z.B., Carvalho, M.H.C., et al. 2008. Increased vascular O-GlcNAcylation augments reactivity to constrictor stimuli. JASH. **2**: 410-417.

Lima, V.V., Giachini, F.R., Carneiro, F.S., Carvalho, M.H., Fortes, Z.B., Webb, R.C., et al. 2011. O-GlcNAcylation contributes to the vascular effects of ET-1 via activation of the RhoA/Rho-kinase pathway. Cardiovasc Res. **89**(3): 614-622.

Lima, V.V., Giachini, F.R., Choi, H., Carneiro, F.S., Carneiro, Z.N., Fortes, Z.B., et al. 2009. Impaired vasodilator activity in deoxycorticosterone acetate-salt hypertension is associated with increased protein O-GlcNAcylation. Hypertension. **53**(2): 166-174.

Lima, V.V., Giachini, F.R., Hardy, D.M., Webb, R.C. and Tostes, R.C. 2011. O-GlcNAcylation: a novel pathway contributing to the effects of endothelin in the vasculature. Am J Physiol Regul Integr Comp Physiol. **300**(2): R236-250.

Lima, V.V., Rigsby, C.S., Hardy, D.M., Webb, R.C. and Tostes, R.C. 2009. O-GlcNAcylation: a novel post-translational mechanism to alter vascular cellular signaling in health and disease: focus on hypertension. Journal of the American Society of Hypertension. **3**(6): 374-387.

Love, D.C. and Hanover, J.A. 2005. The hexosamine signaling pathway: deciphering the "O-GlcNAc code". Sci STKE. **2005**(312): re13.

Martinez-Revelles, S., Avendano, M.S., Garcia-Redondo, A.B., Alvarez, Y., Aguado, A., Perez-Giron, J.V., et al. 2013. Reciprocal relationship between reactive oxygen species and cyclooxygenase-2 and vascular dysfunction in hypertension. Antioxid Redox Signal. **18**(1): 51-65.

Martyn, K.D., Frederick, L.M., von Loehneysen, K., Dinauer, M.C. and Knaus, U.G. 2006. Functional analysis of Nox4 reveals unique characteristics compared to other NADPH oxidases. Cell Signal. **18**(1): 69-82.

Munzel, T., Afanas'ev, I.B., Kleschyov, A.L. and Harrison, D.G. 2002. Detection of superoxide in vascular tissue. Arterioscler Thromb Vasc Biol. **22**(11): 1761-1768.

Musicki, B., Kramer, M.F., Becker, R.E. and Burnett, A.L. 2005. Inactivation of phosphorylated endothelial nitric oxide synthase (Ser-1177) by O-GlcNAc in diabetes-associated erectile dysfunction. Proc Natl Acad Sci U S A. **102**(33): 11870-11875.

Ngoh, G.A., Watson, L.J., Facundo, H.T. and Jones, S.P. 2011. Augmented O-GlcNAc signaling attenuates oxidative stress and calcium overload in cardiomyocytes. Amino Acids. **40**(3): 895-911.

Niu, X.L., Madamanchi, N.R., Vendrov, A.E., Tchivilev, I., Rojas, M., Madamanchi, C., et al. 2010. Nox activator 1: a potential target for modulation of vascular reactive oxygen species in atherosclerotic arteries. Circulation. **121**(4): 549-559.

Olukman, M., Orhan, C.E., Celenk, F.G. and Ulker, S. 2010. Apocynin restores endothelial dysfunction in streptozotocin diabetic rats through regulation of nitric oxide synthase and NADPH oxidase expressions. J Diabetes Complications. **24**(6): 415-423.

Pashkow, F.J. 2011. Oxidative Stress and Inflammation in Heart Disease: Do Antioxidants Have a Role in Treatment and/or Prevention? Int J Inflam. **2011**: 514623.

Rabelo, L.A., Souza, V.N., Fonseca, L.J. and Sampaio, W.O. 2010. Redox unbalance: NADPH oxidase as therapeutic target in blood pressure control. Arq Bras Cardiol. **94**(5): 643-651, 684-693.

Rajapakse, A.G., Ming, X.F., Carvas, J.M. and Yang, Z. 2009. The hexosamine biosynthesis inhibitor azaserine prevents endothelial inflammation and dysfunction under hyperglycemic condition through antioxidant effects. Am J Physiol Heart Circ Physiol. **296**(3): H815-822.

Rehman, A.U., Dugic, E., Benham, C., Lione, L. and Mackenzie, L.S. 2013. Selective inhibition of NADPH oxidase reverses the over contraction of diabetic rat aorta. Redox Biol. **2C**: 61-64.

Ross, R. 1971. The smooth muscle cell. II. Growth of smooth muscle in culture and formation of elastic fibers. J Cell Biol. **50**(1): 172-186.

Satoh, K., Berk, B.C. and Shimokawa, H. 2011. Vascular-derived reactive oxygen species for homeostasis and diseases. Nitric Oxide. **25**(2): 211-215.

Silva, B.R., Pernomian, L., Grando, M.D., Amaral, J.H., Tanus-Santos, J.E. and Bendhack, L.M. 2013. Hydrogen peroxide modulates phenylephrine-induced contractile response in renal hypertensive rat aorta. Eur J Pharmacol. **721**(1-3): 193-200.

Singh, L.P., Cheng, D.W., Kowluru, R., Levi, E. and Jiang, Y. 2007. Hexosamine induction of oxidative stress, hypertrophy and laminin expression in renal mesangial cells: effect of the anti-oxidant alpha-lipoic acid. Cell Biochem Funct. **25**(5): 537-550.

Taye, A., Saad, A.H., Kumar, A.H. and Morawietz, H. 2010. Effect of apocynin on NADPH oxidase-mediated oxidative stress-LOX-1-eNOS pathway in human endothelial cells exposed to high glucose. Eur J Pharmacol. **627**(1-3): 42-48.

Touyz, R.M. and Briones, A.M. 2011. Reactive oxygen species and vascular biology: implications in human hypertension. Hypertens Res. **34**(1): 5-14.

Touyz, R.M. and Schiffrin, E.L. 2008. Reactive oxygen species and hypertension: a complex association. Antioxid Redox Signal. **10**(6): 1041-1044.

Yamada, J., Yoshimura, S., Yamakawa, H., Sawada, M., Nakagawa, M., Hara, S., et al. 2003. Cell permeable ROS scavengers, Tiron and Tempol, rescue PC12 cell death caused by pyrogallol or hypoxia/reoxygenation. Neurosci Res. **45**(1): 1-8.

Yang, J., Su, Y. and Richmond, A. 2007. Antioxidants tiron and N-acetyl-L-cysteine differentially mediate apoptosis in melanoma cells via a reactive oxygen species-independent NF-kappaB pathway. Free Radic Biol Med. **42**(9): 1369-1380.

Zeidan, Q. and Hart, G.W. 2010. The intersections between O-GlcNAcylation and phosphorylation: implications for multiple signaling pathways. J Cell Sci. **123**(Pt 1): 13-22.

LEGEND TO FIGURES

Figure 1: O-GlcNAc levels are increased in VSMC after PUGNAc incubation. A) O-GlcNAc levels were evaluated in VSMC incubated with vehicle (methanol, white bar) or PUGNAc (100 μM; black bars) for 15 min, 30 min, 1 h, 6 h or 24 h. Results are expressed as mean ± SEM. n = 5-6, for each experimental group. * $P \leq 0.05$ vs. vehicle. (One-way analysis of variance, followed by post hoc comparisons using the Newman-Keuls test). B) Phase contrast microscopy demonstrating that treatment with PugNAc (bottom pictures) increases O-GlcNAc-proteins in cultured VSMCs. Blue, DAPI stained nuclei; green, O-GlcNAc-modified proteins [FITC-labeled second antibody (anti-mouse IgG) and primary anti-O-GlcNAc. Magnification x20.

Figure 2. **O-GlcNAc decreases endothelium-dependent relaxation in aorta, an effect prevented by apocynin and Tiron.** Concentration-response curves to ACh, to assess endothelium-dependent relaxation, were performed in aortic segments incubated with vehicle (methanol, white square) or PUGNAc, in the absence (white circle) or presence of apocynin (black square) or Tiron (black circle). n = 6 for each experimental group. Results are expressed as mean ± SEM. Experimental values of the relaxation induced by ACh were calculated relative to the maximal changes from the contraction produced by PE, which was taken as 100%. * $P \leq 0.05$ vs. vehicle. (One-way analysis of variance, followed by post hoc comparisons using the Newman-Keuls test).

Figure 3. Increased O-GlcNAc levels positively modulate ROS generation in aortic segments. Frozen aortic sections were incubated with Dihydroethidium (DHE, 50 mM, green) for 30 min to evaluate ROS generation (red). **A)** Fluorescence measurement charts in each experimental condition: vehicle (white bar), incubation with PUGNAc (black bars, 12 or 24 h) or with Ang II (chess bar, 30 min). **B)** Representative photos of each

assessed group. **C)** PUGNAc effect on $\bullet O_2^-$ generation was assessed with lucigenin, after 12 or 24 h of stimulation. Results are expressed as mean ± SEM. n = 5 for each experimental group. * $P \leq 0.05$ vs. vehicle (methanol); † $P \leq 0.05$ vs. PUGNAc 12 h. (Analysis of variance and Student's t-test, post hoc comparisons were performed by the Newman-Keuls).

Figure 4. O-GlcNAc increases Nox-1 and Nox-4 protein expression both in aorta and VSMC. Aortas (A and B) or VSMCs (C and D) were incubated with vehicle (methanol, white bar) or PUGNAc (black bar; 6, 12 or 24 h). Protein expression of **A**) Nox-1 and **B**) Nox-4 in rat thoracic aortas, and **C**) Nox-1 and **D**) Nox-4 in VSMCs, was determined. Results are expressed as mean ± SEM. n = 4-5 for each experimental group. * $P \leq 0.05$ vs. vehicle. (Analysis of variance and Student's t-test, post hoc comparisons were performed by the Newman-Keuls).

Figure 5. O-GlcNAc increases translocation of $p47^{phox}$ from the cytosol to the membrane: NADPH activity in aorta. Aortas were incubated with vehicle (methanol, white bar) or PUGNAc (black bars; 12 h) and subjected to ultracentrifugation protocols to isolate membrane and cytosolic fractions. **A**) representative photos and **B**) quantification of $p47^{phox}$ protein expression in the membrane over cytosolic fractions. Results are expressed as mean ± SEM. n = 4-5 for each experimental group. * $P \leq 0.05$ vs. vehicle. (One-sample t test).

Figure 6. O-GlcNAc increases $p22^{phox}$ protein expression in VSMCs. VSMCs were incubated with vehicle (methanol, white bar) or PUGNAc (black bar; 6, 12 or 24 h) and $p22^{phox}$ protein expression was determined. On the top, representative Western blot images of $p22^{phox}$ and β-actin; on the bottom, bar graph show the relative $p22^{phox}$ proteins after

normalization to β-actin expression. Results are expressed as mean ± SEM. n = 4-5 for each experimental group. * $P \leq 0.05$ vs. vehicle. (Analysis of variance and Student's t-test, post hoc comparisons were performed by the Newman-Keuls).

LEGEND TO TABLES

Table I. E_{max} and pD_2 values for ACh in rat aortas incubated with vehicle or PUGNAc, in the presence or absence of apocynin or Tiron (24 h).

Group	E_{max}	pD_2
Vehicle	94.1 ± 1.9	7.3 ± 0.07
PUGNAc	77.8 ± 3.1*	6.6 ± 0.10*
PUGNAc + apocynin	86.8 ± 2.2 †	7.5 ± 0.10 †
PUGNAc + Tiron	88.0 ± 2.5 †	7.2 ± 0.10 †

Results are presented as mean ± SEM (n = 6 in each group). The potency of the agonist is expressed as pD_2 (negative logarithm of the molar concentration that produces 50% maximal response). Sigmoidal curves were drawn to determine the pD_2 values. Statistical significance of data was determined by analysis of variance (ANOVA one-way) followed by the Newman-Keuls post-test * $P < 0.05$ vs. vehicle. † $P < 0.05$ vs. PUGNAc.

Figure 1

Figure 1A

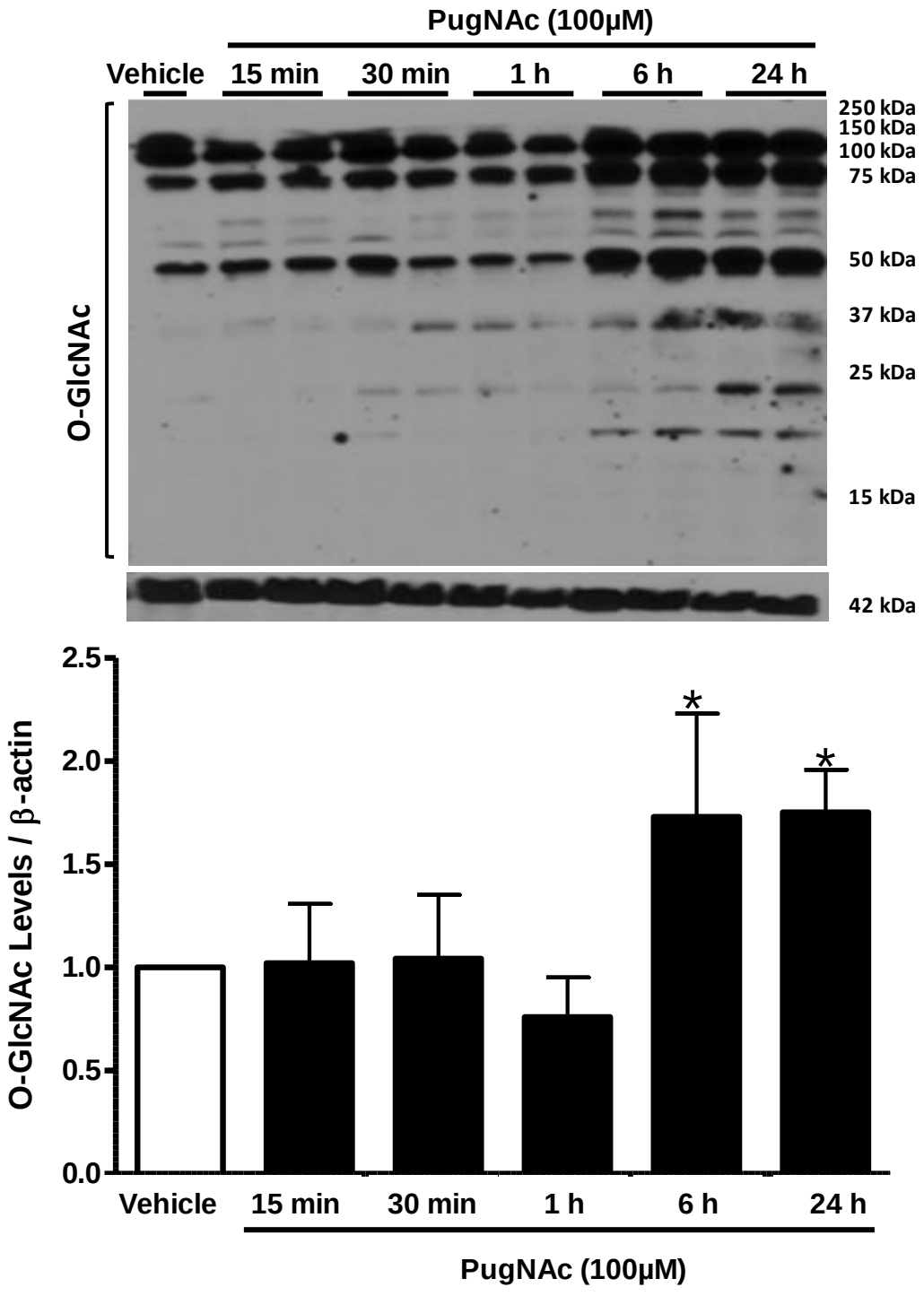

Figure 1B

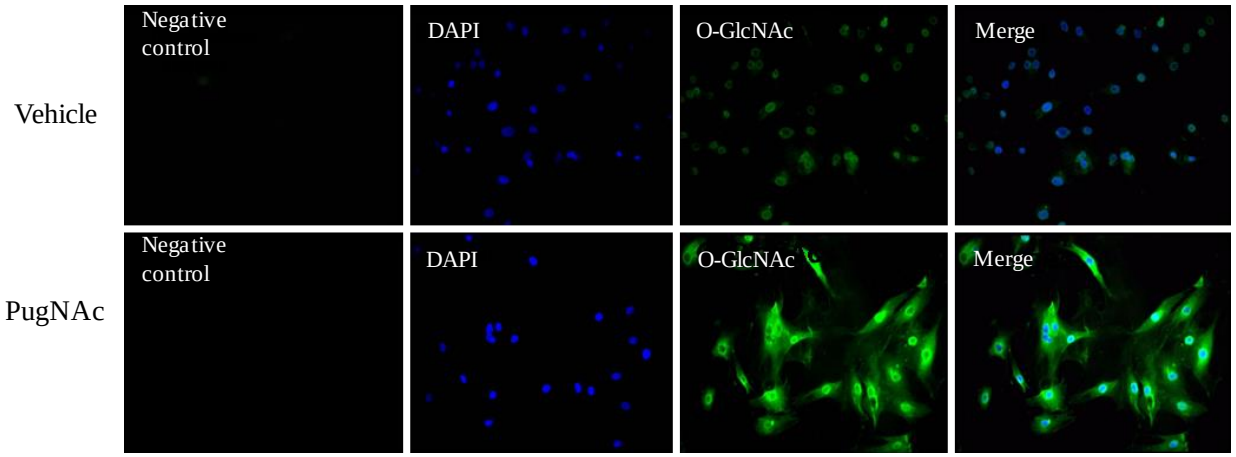
Vehicle
PugNAc
Negative control
DAPI
O-GlcNAc
Merge
Negative control
DAPI
O-GlcNAc
Merge

Figure 2

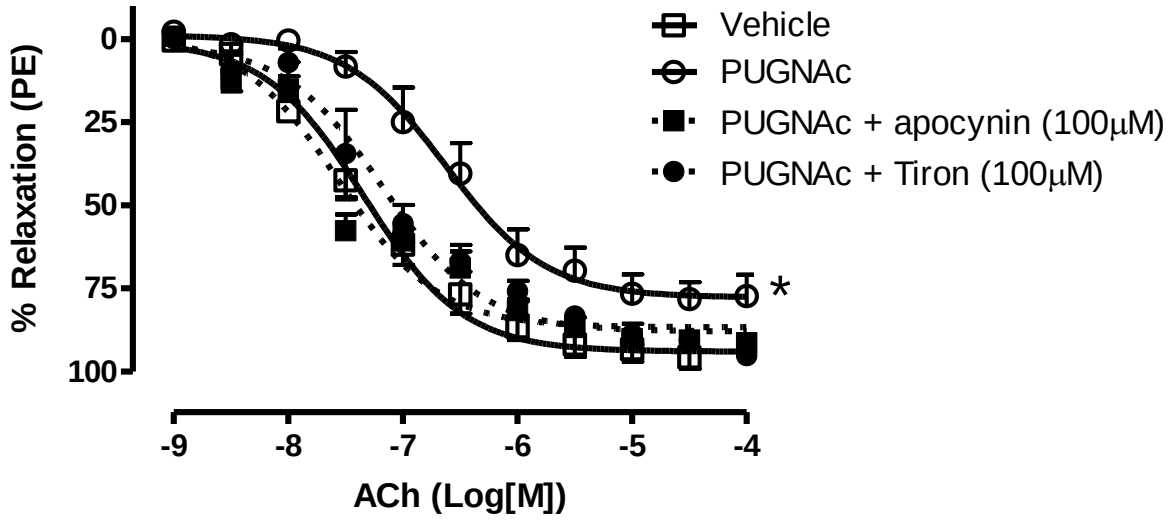
Vehicle
PUGNAc
PUGNAc + apocynin (100μM)
PUGNAc + Tiron (100μM)
% Relaxation (PE)
0
25
50
75
100
-9
-8
-7
-6
-5
-4
ACh (Log[M])
*

Figure 3

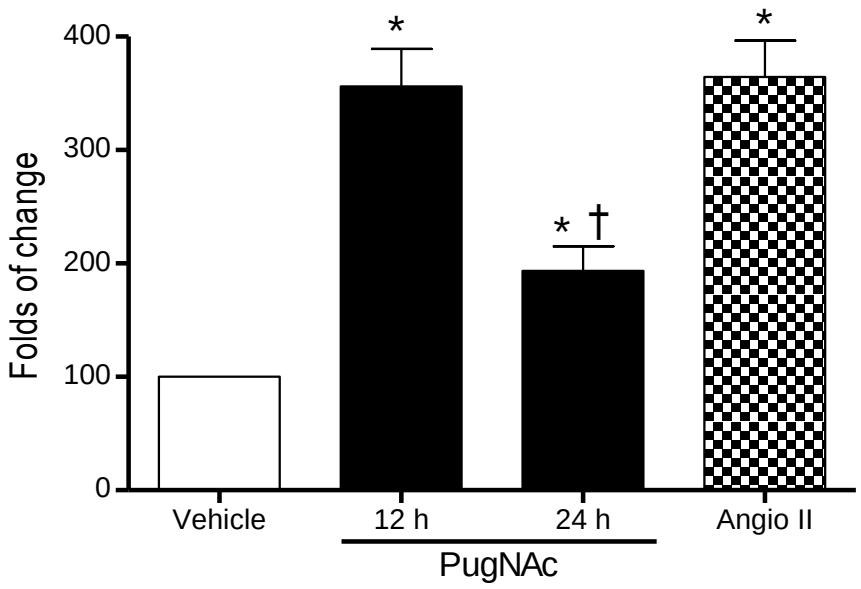
400
300
200
100
0
Folds of change
*
*
* †
Vehicle
12 h
24 h
Angio II
PugNAc

Figure 3B

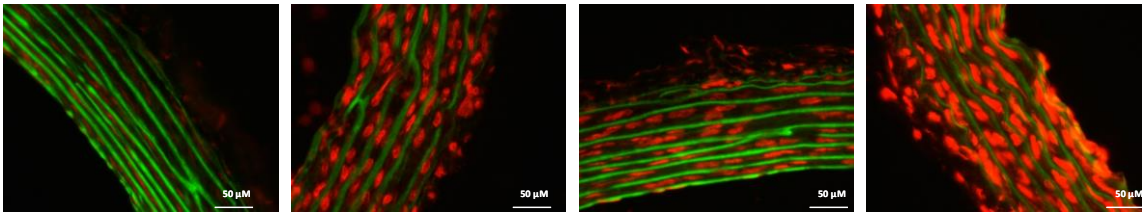

Vehicle | PUGNAc -12 h | PUGNAc - 24 h | Ang II – 30 min

Figure 3C

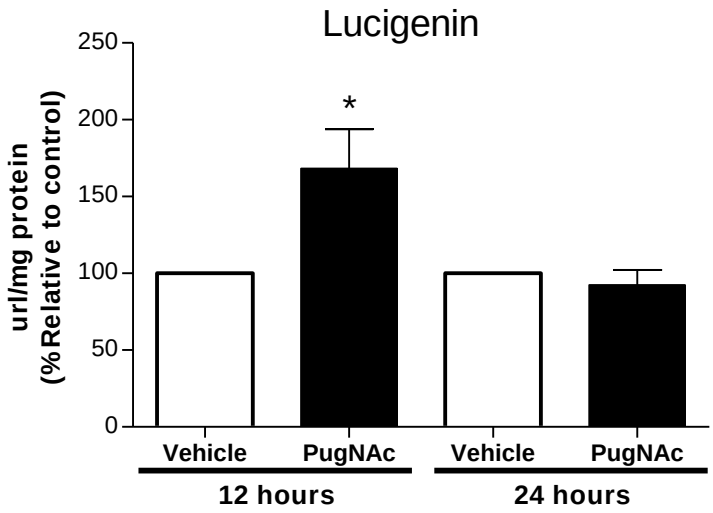

Figure 4

AORTA

Figure 4A

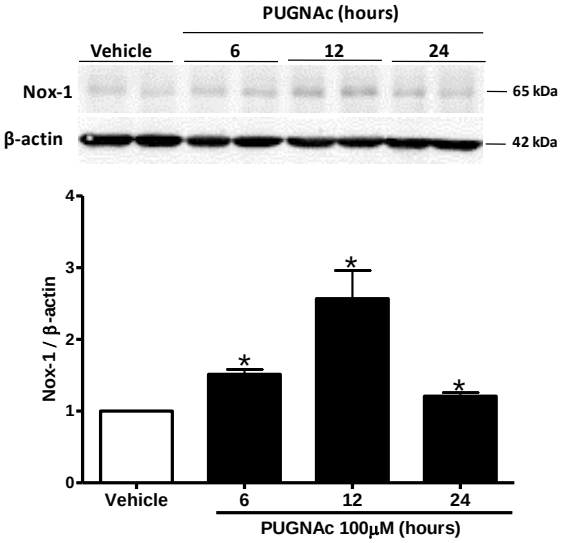

Figure 4B

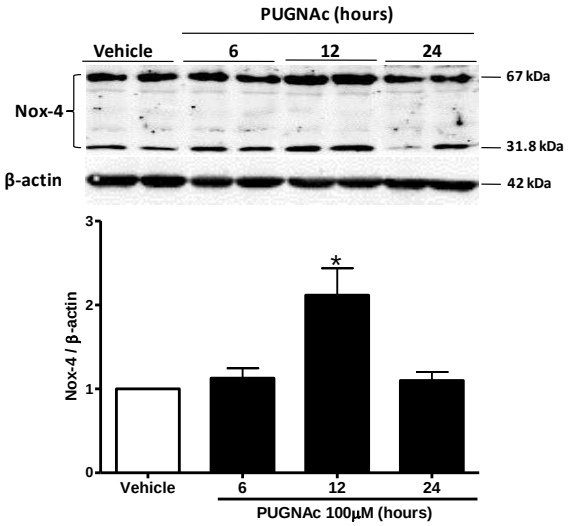

VSMC

Figure 4C

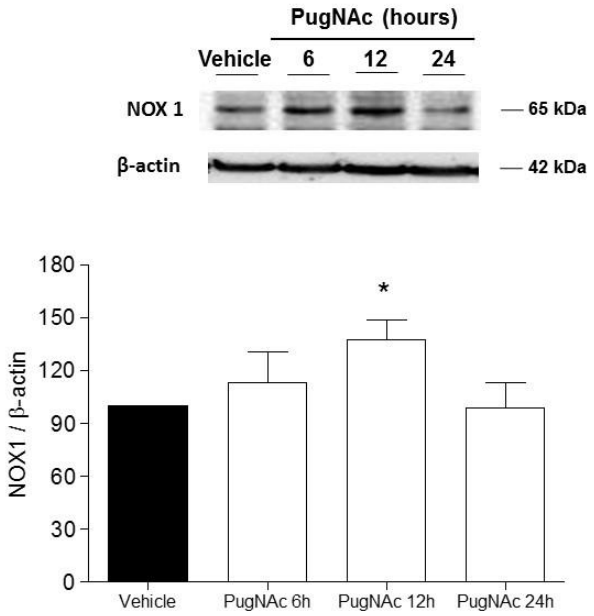

Figure 4D

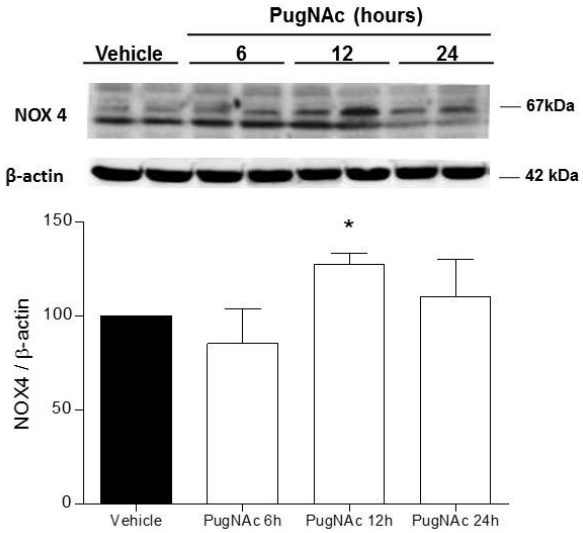

Figure 5

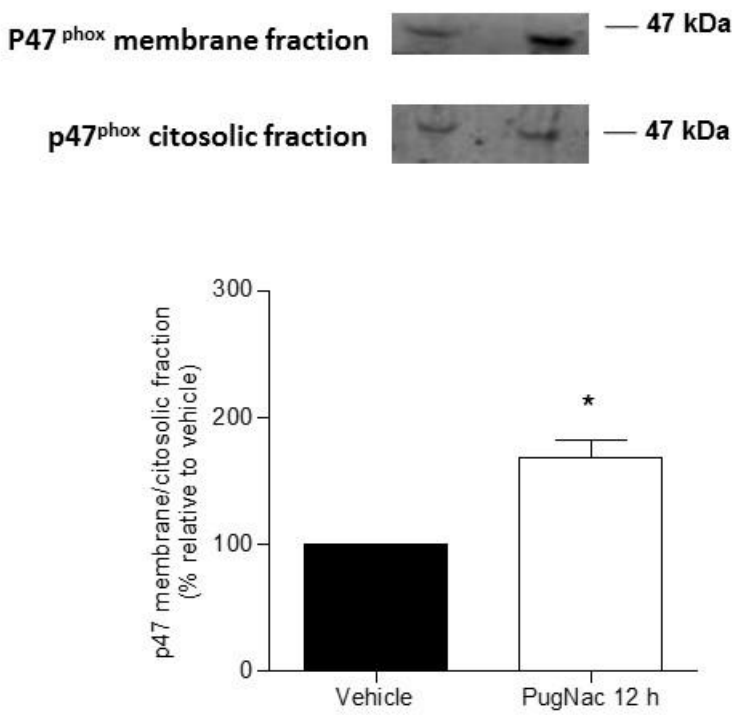
P47 phox membrane fraction
47 kDa
p47phox citosolic fraction
47 kDa
p47 membrane/citosolic fraction
(% relative to vehicle)
300
200
100
0
*
Vehicle
PugNac 12 h

Figure 6

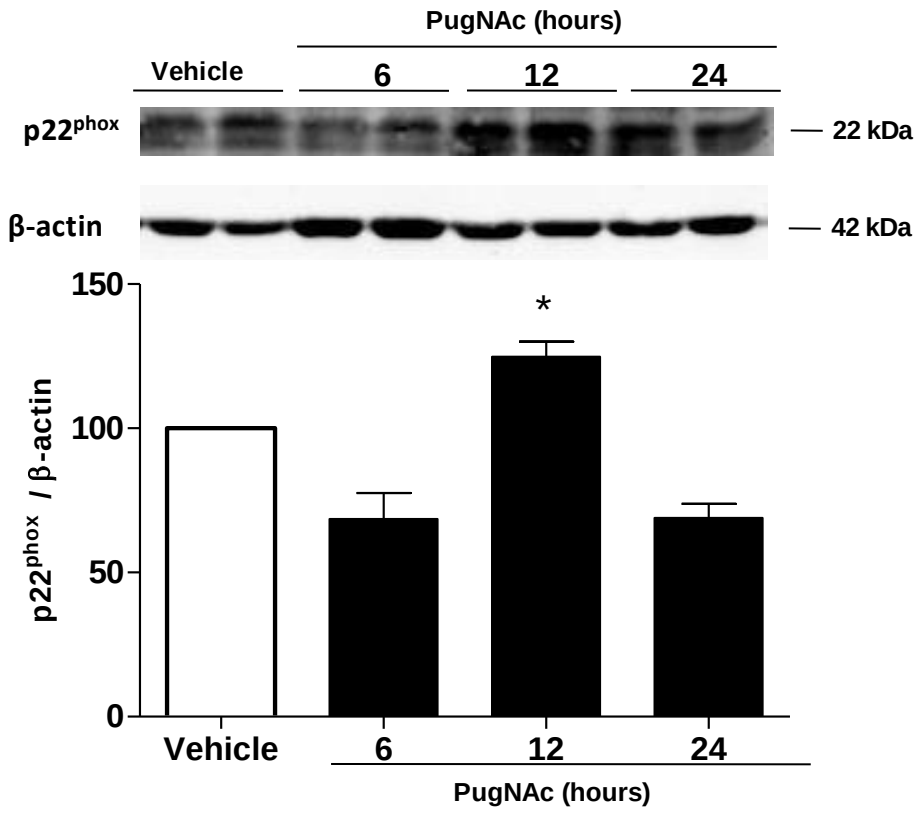
PugNAc (hours)
Vehicle
6
12
24
p22phox
22 kDa
β-actin
42 kDa
150
100
50
0
p22phox / β-actin
*
Vehicle
6
12
24
PugNAc (hours)